Article

Widespread Involvement of Acetylation in the Retinal Metabolism of Form-Deprivation Myopia in Guinea Pigs

Jiaojiao Feng, Xiuyan Zhang, Runkuan Li, Ping Zhao, Xudong Han, Qiuxin Wu, Qingmei Tian, Guodong Tang, Jike Song,* and Hongsheng Bi*

Read Online

ACCESS | 📊 Metrics & More | 📖 Article Recommendations | 🆘 Supporting Information
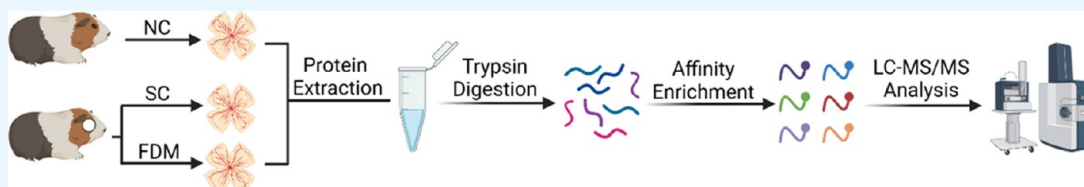
ABSTRACT: Myopia has become the major cause of visual impairment worldwide. Although the pathogenesis of myopia remains controversial, proteomic studies suggest that dysregulation of retinal metabolism is potentially involved in the pathology of myopia. Lysine acetylation of proteins plays a key role in regulating cellular metabolism, but little is known about its role in the form-deprived myopic retina. Hence, a comprehensive analysis of proteomic and acetylomic changes in the retinas of guinea pigs with form-deprivation myopia was performed. In total, 85 significantly differential proteins and 314 significantly differentially acetylated proteins were identified. Notably, the differentially acetylated proteins were markedly enriched in metabolic pathways such as glycolysis/gluconeogenesis, the pentose phosphate pathway, retinol metabolism, and the HIF-1 signaling pathway. HK2, HKDC1, PKM, LDH, GAPDH, and ENO1 were the key enzymes in these metabolic pathways with decreased acetylation levels in the form-deprivation myopia group. Altered lysine acetylation of key enzymes in the form-deprived myopic retina might affect the dynamic balance of metabolism in the retinal microenvironment by altering their activity. In conclusion, as the first report on the myopic retinal acetylome, this study provides a reliable basis for further studies on myopic retinal acetylation.

INTRODUCTION

Myopia is a refractive error in which light entering the eye parallel to the visual axis forms a focal point in front of the retina when the ciliary muscle is relaxed.[1] As a result of hyperextension of the eyeball, myopia has become one of the leading causes of visual impairment worldwide.[2] According to a meta-analysis, almost half of the world's population may be myopic by 2050, with as much as 10% of the population being highly myopic.[3] This is of particular concern because patients with high myopia have the potential to develop pathological myopia and related vision-threatening eye diseases, including posterior scleral staphyloma, myopia-related optic neuropathy, retinal choroidal atrophy, and myopic macular degeneration.[4,5] Therefore, more research is needed on the pathogenesis of myopia to develop interventions that can slow the progression.[6]

A diffuser that causes blurring of images on the retina is used in experimental studies of myopia, thereby inducing axial elongation of the eye, known as form-deprivation myopia (FDM).[7] In many respects, the FDM model has become one of the most useful experimental models in myopia research. As the first station for the perception of visual signals, the retina plays a substantial role in the aetiology of myopia. The results of animal model studies have confirmed the presence of visual regulation of eye growth and refractive development as well as local retinal control of eye growth.[8] In recent years, numerous studies on retinal regulatory mechanisms have detailed the various molecular mechanisms involved in the development of FDM, including neurotransmitters,[9] noncoding RNAs,[10] and cellular functions.[11] Due to advances in biological techniques, proteomic analysis has become a viable approach to reveal the underlying molecular mechanisms of myopia in their entirety.[12−15] We found multiple studies identifying molecules and pathways associated with metabolism in the myopic retina, including insulin expression,[13] apo A1 expression,[14] glycolysis, and mitochondrial metabolism.[15] However, the molecular mechanism of retinal metabolic dysregulation due to myopia is still elusive.

Post-translational modification (PTM) is a critical step in protein biosynthesis that alters the properties and functions of proteins by adding, folding, or removing functional groups.[16]

Protein lysine acetylation (Kac) is one of the key PTMs in eukaryotes and is regulated by two types of enzymes, lysine acetyltransferases and lysine deacetylases, which are responsible for the addition and removal of acetyl groups, respectively.[17] In 1964, Allfrey and colleagues first identified the acetylation of histones, which was mainly associated with chromatin remodeling and transcriptional activation.[18] In addition, proteomic studies have revealed the possibility of acetylation of thousands of nonhistone proteins, including those involved in processes such as ATP binding, transporter activity, structural components of the cytoskeleton, and protein folding.[17,19] In functional studies of acetylation modifications, numerous reports have suggested that acetylation has a vital role in the regulation of metabolism.[20−23] Zhao et al. characterized 1047 acetylated proteins in human liver tissue and found that almost all enzymes involved in the TCA cycle, glycolysis, and fatty acid metabolism were acetylated.[21] One of the key enzymes in the pentose phosphate pathway is glucose-6-phosphate dehydrogenase (G6PD), and studies have shown that G6PD activity is negatively regulated by lysine 403 (K403) acetylation, which impairs the formation of catalytically active dimers.[22] Glutathione is a key component of the antioxidant system, preventing the toxic effects of reactive oxygen/nitrogen species on cells. Pehar et al. found a decrease in glutathione levels associated with increased Kac in a mouse model of amyotrophic lateral sclerosis.[23]

To date, proteomic studies of FDM have revealed several molecules and pathways associated with retinal metabolism, yet their regulatory mechanisms remain unclear. In recent years, the Kac of proteins has been recognized as a key PTM in the regulation of cellular metabolism, and its role in retinal metabolic dysregulation in FDM is unknown. Therefore, this study provides the first comprehensive proteomic and acetylated proteomic analysis of the guinea pig retina in FDM, and it aims to provide new perspectives on the mechanisms of retinal regulation in myopia. This study provides valuable data to support further exploration of biomarkers and therapeutic targets for myopia.

■ METHODS

Form-Deprivation Myopia in Guinea Pigs. Two-week-old male tricolored guinea pigs (*Cavia porcellus*, 90−110 g) were acquired from Henan Kangda Experimental Animal Co., Ltd. and housed in plastic cages (54.5 × 39.5 × 20 cm^3) with 5 animals per cage in a temperature- and humidity-controlled room. The illumination level in the animal room was ~350 lux, with a daily lighting/darkness cycle every 12 h. Water and feed were provided *ad libitum* along with fresh vegetables twice a day. The Animal Care and Use Committee of the Shandong Academy of Eye Disease Prevention and Therapy approved this experiment, and all animal treatments and care were in accordance with the Association for Research in Vision and Ophthalmology (ARVO) Statement on the Use of Animals in Ophthalmic and Vision Research.

Thirty guinea pigs were randomly divided into 3 groups: normal control (NC, n = 15), form-deprivation myopia (FDM, n = 15), and self-control (SC, n = 15). Animals in the NC group had both eyes exposed normally in the absence of any treatment. A 3D-printed hood modified with a latex balloon with 60% light transmission was placed over the head of guinea pigs in the FDM group for animal experiments.[24] The hood covered only the right eyes of the guinea pigs, leaving the left eyes, noses, mouths, and ears uncovered. The uncovered left eyes served as the SC group. The right eyes of the guinea pigs were completely covered by the hood, but the hood was not in contact with the corneas and eyelids. Animals were checked 3 times a day during 12 h of daylight to ensure that the hoods were in position and clean and promptly changed to the right size if necessary.

Refractive Status and Ocular Biometrics. The protocols for measuring refractive status and ocular axis in this study were consistent with previous reports.[24] Briefly, refractive error and axial length (AL) were measured at 0, 1, and 2 weeks using hand-held streak retinoscopy (YZ24; Six Six Vision Technology Co., Ltd., Suzhou, China) and high-frequency A-scan ultrasonography (11 MHz, Cinescan, Quantel Medical, France), respectively. The refraction was calculated with the average of the vertical and horizontal diameters of 3 repeated measurements. For AL measurement, the average of 10 repeated measurements was taken. The hoods of the animals in the FDM group were removed before and replaced immediately after the measurement.

Retina Collection and Protein Extraction. After 2 weeks of form deprivation, guinea pigs were executed by overdose of barbiturates. After deep anesthesia, the eyes were rapidly scooped out of their sockets. After clipping the extraocular tissues, a circular cut was made near the corneal rim, and the anterior portion was discarded. The retina without choroidal tissue attachment was isolated from the posterior segment for harvesting. Then, the retina was rapidly transferred to liquid nitrogen and stored in a −80 °C fridge until use.

Retinas were removed from storage at −80 °C, powdered with liquid nitrogen, and shifted to a 5 mL centrifuge tube. Subsequently, the powder was added to 4 volumes of lysis buffer containing 1% protease inhibitor cocktail. The remaining debris was removed by centrifugation at 12 000g for 10 min at 4 °C using a high-intensity sonicator. Lastly, the supernatant was collected and the protein concentration was determined using a dicinchoninic acid kit.

Western Blotting Analysis. After homogenization and protein concentration determination, three separate samples from each group with adequate and similar protein concentrations were selected for acetylation-modified protein Western blot filter analysis. Twenty micrograms of protein lysate was separated by 12% SDS-PAGE and electrotransferred onto poly(vinylidene fluoride) membranes (Merck Millipore, Tullagreen, Ireland) at 300 V, 200 mA for 110 min. The membrane layer was closed with 5% skimmed milk powder at 4 °C for 1 h. The membranes were then incubated with an antiacetylation antibody (1:500; PTM-105RM, PTM Bio, Hangzhou, China) overnight. The membranes were washed with Tris-buffered saline with Tween-20 (TBST) three times for 10 min each. Afterward, the membranes were incubated with horseradish peroxidase (HRP)-coupled secondary antibody (1:10 000; 31460, Thermo) for 2 h at 4 °C. After three more washes with TBST, the protein bands were visualized with the ECL kit.

Trypsin Digestion and Panantibody-Based PTM Enrichment. Six retinas from each group were selected for protein extraction. Protein digestion and enrichment of acetylated peptides were performed regarding previous descriptions.[25] Trypsin digestion was performed with 5 mM dithiothreitol for 30 min at 56 °C and with 11 alkylated mM iodoacetamide for 15 min in darkness at room temperature. The protein samples were diluted in 0.1 M triethylammonium bicarbonate (TEAB), and urea (less than 2 M) was added.
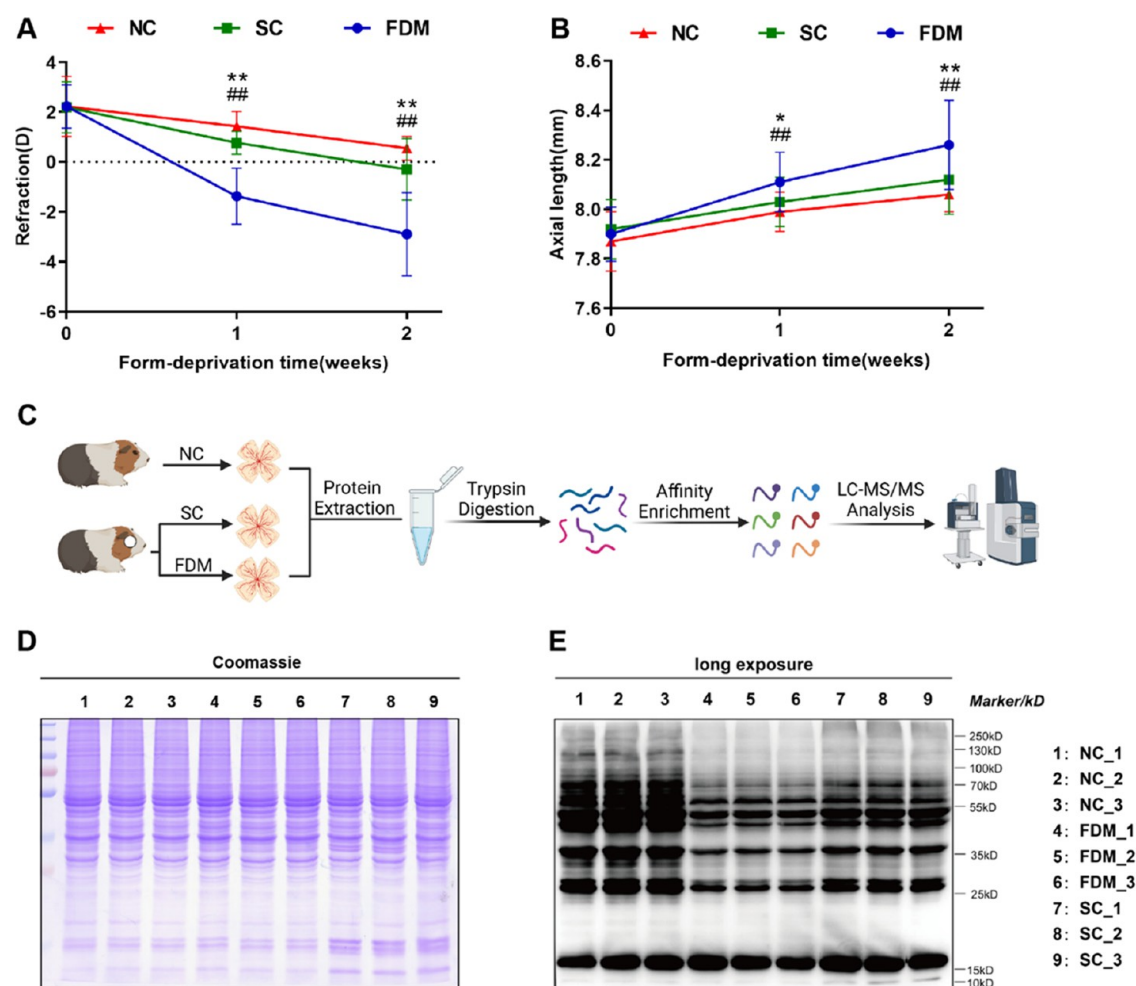
Figure 1. Outline of the experiments. Changes in refraction (A) and AL (B). *$p < 0.01$ and **$p < 0.001$ for the NC group versus the FDM group at the same time point. #$p < 0.01$ and ##$p < 0.001$ for the SC group versus the FDM group. (C) Schematic of the LC/MS-based quantitative acetyl proteomic strategy. (D, E) Western blotting of proteins in three groups of retinas with antilysine acetylation antibodies. Coomassie brilliant blue-stained (D) and long exposure (E) images.

Finally, trypsin was added overnight for the first digestion at a trypsin-to-protein mass ratio of 1:50 and for the second digestion for 4h at a trypsin–protein mass ratio of 1:100.

The acetylated peptides were enriched as described by Wan et al.[25] Briefly, the peptides were first dissolved in NETN buffer and incubated with an antiacetylation antibody overnight. The resin was then washed four times with buffer and two times with deionized water. The bound peptide was eluted 3 times with 0.1% trifluoroacetic acid. Finally, the peptides were desalted according to the instructions of C18 ZipTips, vacuum freeze-dried, and then analyzed by LC-MS.

LC-MS/MS and Database Analysis. LC-MS/MS analysis and database search based on previous reports.[26] Briefly, tryptic peptides were dissolved in a mixture of 0.1% formic acid and 2% acetonitrile in water and directly sampled onto a reversed-phase precolumn. Next, the peptides were separated using an EnanoElute UHPLC system (Bruker Daltonics) at a fixed flow rate of 450 nL/min as follows: mobile phase B consisted of an aqueous solution containing 0.1% formic acid in acetonitrile, and the liquid gradient was set to 0–70 min, 6–24%; 70–84 min, 24–35%; 84–87 min, 35–80%; and 87–90 min, 80%. Subsequently, MS analysis was conducted with a timsTOF Pro system (Bruker Daltonics), which was acquired in parallel accumulation-sequence fragmentation (PASEF)

mode. Precursors with charge states of 0–5 were cleaved, and 10 PASEF-MS/MS scans were acquired per cycle. The dynamic exclusion parameter was set to 30 s.

The resulting MS/MS data were processed using the MaxQuant search engine (v.1.6.15.0). Tandem mass spectra of guinea pigs (*C. porcellus*) were searched in the UniProt database. For quantitative proteomic data, the mass tolerance of precursor ions was set as 20 ppm; in the main search, it was set as 5 ppm; and the mass tolerance of fragment ions was set as 0.02 Da. The error detection rate (FDR) was set at less than 1%. For the acetylated proteome, the maximum leaky cleavage of trypsin/P was set to 4. The mass error of the precursor ion was set to 10 ppm, while the mass error was set to 0.02 Da for the fragment ion. Carbamoyl methylation on Cys was considered as a fixed modification, whereas the variable modifications were acetylation of lysine and oxidation of Met. The FDR threshold for proteins, peptides, and modification sites was set to 0.01. The minimum peptide length was set to 7, and the site positioning probability was set to >0.75.

Bioinformatic Analysis. First, we used WoLF PORT software (http://wolfpsort.org/) to analyze protein subcellular localization. Functional enrichment analysis of the functions and pathways involved in the proteins was then performed,
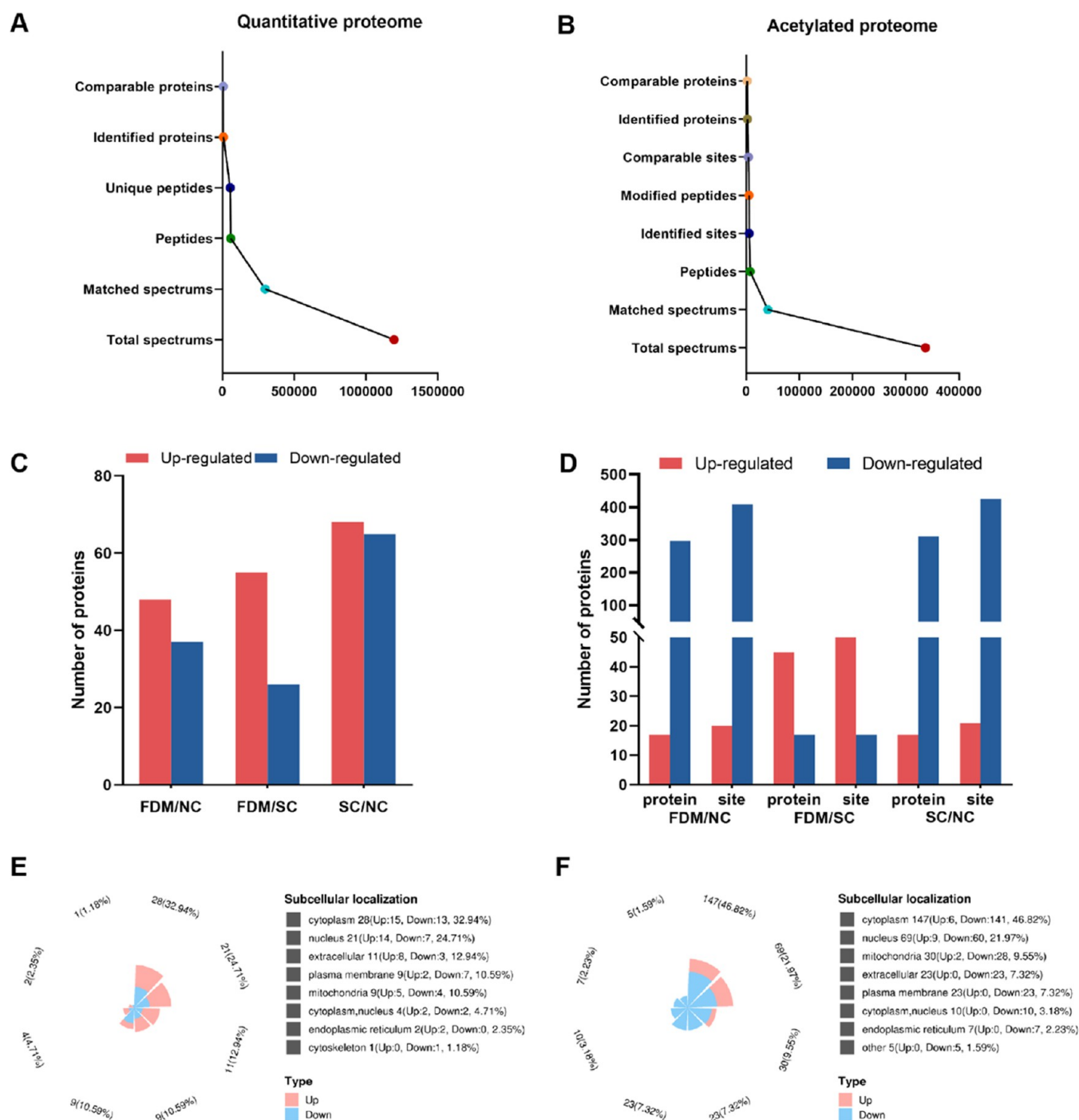
Figure 2. Analysis of the quantitative proteome and acetylated proteome. (A) Overview map of the identified proteins in the quantitative proteome. (B) Overview map of the identified acetylated proteins in the acetylated proteome. (C) Histogram of the number of differential proteins in the quantitative proteome. (D) Histogram of the number of differentially acetylated proteins and sites in the acetylated proteome. (E) Rose plot of subcellular localization of differential proteins in the FDM versus NC groups. (F) Rose plot of subcellular localization of differentially acetylated proteins in the FDM versus NC groups.

including gene ontology (GO) functional enrichment, Kyoto Encyclopedia of Genes and Genomes (KEGG) pathway, and protein domain analysis. Fisher's exact test was also used to examine the degree of enrichment of differentially expressed proteins. Adjusted *p* values <0.05 are considered significant in all enrichment analyses.[25] The software motif-x was used to analyze a sequence model of the amino acid (aa) composition at specific positions in all acetylated proteins (10 aa upstream and downstream of the modification site). Protein−protein

interactions (PPI) of the identified differentially acetylated proteins were analyzed using the STRING database (v.11.5) and Cytoscape software (v.3.7.0). Densely linked regions were screened and assigned scores using Molecular Complex Detection (MCODE).

Statistical Analysis. Data were all presented as mean ± standard deviation (SD). SPSS 25.0 was used for statistical analysis of experimental data, and GraphPad Prism 8.0 was used for graphing. Differences between the FDM group, the
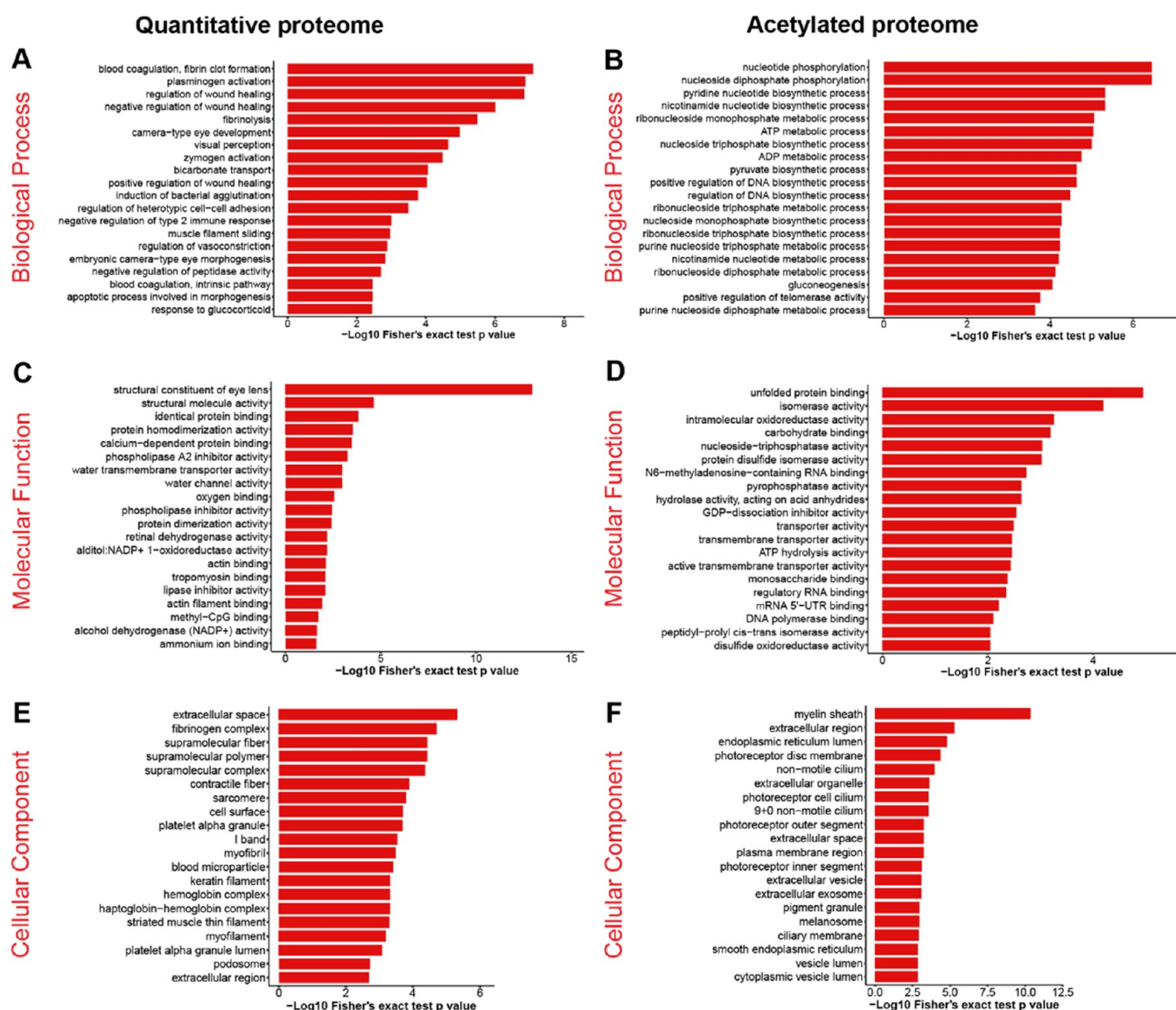
Figure 3. GO functional enrichment. Bar graphs of GO enrichment analysis in the quantitative proteome from biological processes (A), molecular functions (C), and cellular components (E). Bar graphs of GO enrichment analysis in the acetylated proteome from biological processes (B), molecular function (D), and cellular component (F).

SC group, and the NC group at the baseline were assessed using one-way ANOVA, while the LSD-*t* test was used for multiple comparisons between groups. At subsequent time points, paired-sample *t* test or independent *t* test was conducted to assess the significance of the differences between the two groups. *p* values less than 0.05 were considered a statistically significant difference.

■ RESULTS

Form-Deprivation Myopia. No statistically significant difference in refraction or AL was noted among the three groups at the baseline (all *p* > 0.05). After 2 weeks of form deprivation, a significant myopic shift in refraction (−2.90 ± 1.67 D, *p* <0.001; Figure 1A) and AL (8.26 ± 0.18 mm, *p* < 0.001; Figure 1B) was observed in the eyes of the FDM group relative to the NC group and SC group.

Validation Test of Kac Levels. In the present study, we first measured the Kac levels in the three groups of total retinal protein samples using Western blotting and found that the

retinal Kac levels were significantly lower in the FDM and SC groups, especially among the nonhistone proteins (Figure 1D,E). These results suggest that retinal acetylation levels are reduced by form deprivation and provide a hypothesis that reduced retinal lysine acetylation levels are involved in and may contribute to the development of FDM. We next mixed six retinal tissues from each of the three groups to further characterize the differences in lysine acetylation sites of the proteins, as shown in Figure 1C.

Basic Analysis of the Quantitative and Acetylated Proteome. In this study, we performed a comprehensive proteomic and lysine acetylation proteomic analysis of proteins in the retinas of three groups. Principal component analysis (PCA) was used to validate the consistency of the MS data (Figure S1). Furthermore, most of the peptides were between 7 and 20 aa in length, consistent with the general pattern of enzymatic and mass spectrometry-based fragmentation approaches (Figure S2). We identified 6568 proteins, of which 5483 were quantitatively comparable (Figure 2A and Table
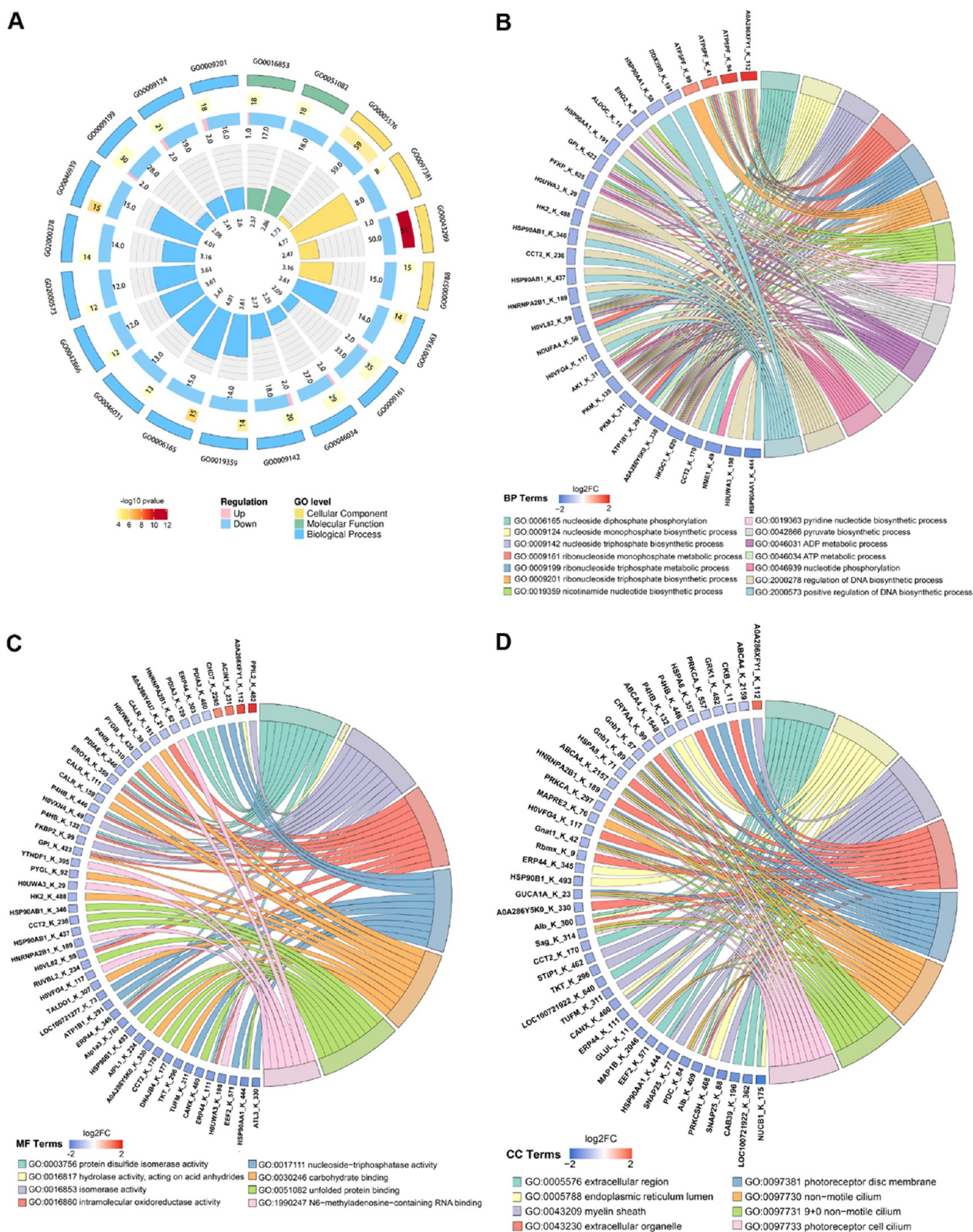
Figure 4. GO functional enrichment of differentially acetylated proteins. (A) Circos plot of acetylated proteins for GO functional enrichment. (B) Chord diagram of the biological processes with acetylated protein enrichment. (C) Chord diagram of the molecular function with acetylated protein enrichment. (D) Chord diagram of cellular components with acetylated protein enrichment.
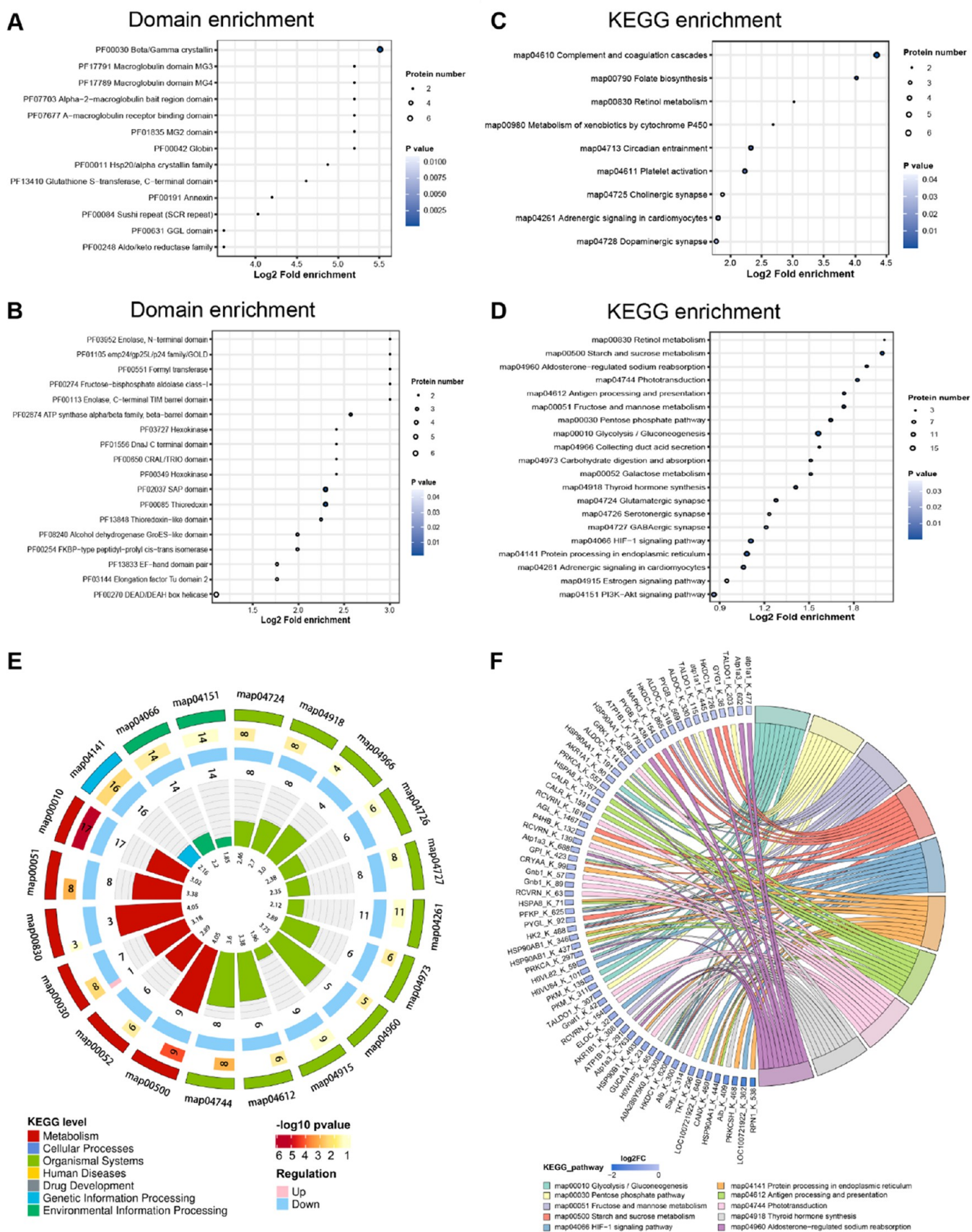
Figure 5. Protein domain and KEGG pathway enrichment for quantitative proteomics and acetylated proteomics. (A) Protein domain analysis of the differential proteins. (B) Protein domain analysis of the differentially acetylated proteins. (C) KEGG pathway enrichment analysis of the differential proteins. (D) KEGG pathway enrichment analysis of the differentially acetylated proteins. (E) Circos plot of acetylated proteins for KEGG pathway enrichment. (F) Chord diagram of KEGG pathway enrichment for differentially acetylated proteins.

S1). MS data showed that 5677 acetylation sites were identified on 2318 proteins, of which 1953 proteins could be compared. (Figure 2B and Table S2).

In quantitative proteomic analysis, the thresholds for selecting differential proteins were fold change ≥1.30 or ≤1/1.3 (Table S3), whereas in the acetylated proteome, fold change ≥1.50 or ≤1/1.5 was used as thresholds for differential change (Table S4). Using this standard, Figure 2C shows differential proteins in the quantitative proteome, and Figure 2D shows differentially acetylated proteins and sites. Heat maps could be applied to visualize the reproduction of differentially expressed proteins in the three replicate samples in quantitative proteomics and acetylomics (Figure S3). Among the 6568 identified proteins, 85 proteins were observed to be differentially expressed in the FDM compared to the NC group, with 48 proteins upregulated and 37 proteins downregulated in the FDM group (Figure 2C). For acetylated proteins, a total of 20 sites with higher acetylation levels and 408 sites with lower acetylation corresponding to 17 upregulated and 297 downregulated proteins were identified in the FDM group (Figure 2D).

Furthermore, site-specific heatmap analysis revealed a clear delineation between the FDM and NC groups, implying that form deprivation resulted in a significant change in the level of acetylation among these proteins (Figure S3). Notably, the changes in the acetylation modification levels in the SC group followed the same trend as those in the FDM group, but their levels increased or decreased to a lesser extent compared to the corresponding form-deprivation eyes. Therefore, to explore the changes in acetylation modifications caused by form deprivation, we will focus on describing the results of the FDM group compared to the NC group, while the results of the other two subgroups are presented in the Supporting Information.

Subcellular Functional Localization. Proteins in eukaryotic tissue cells were localized to various intracellular components based on differences in the structure of the membrane to which they bind. Based on this, we used WolF Psort software for the subcellular structure annotation of proteins. Subcellular localization analysis revealed that in the quantitative proteome, the majority of the differential proteins were located in the cytoplasm (32.94%), nucleus (24.71%), extracellular components (12.94%), and mitochondria (10.59%) (Figure 2E), while differentially acetylated proteins were mainly located in the cytoplasm (46.82%), nucleus (21.97%), and mitochondria (9.55%) (Figure 2F). Notably, upregulated acetylated proteins were primarily distributed in the nucleus (52.94%), whereas downregulated acetylated proteins were primarily distributed in the cytoplasm (47.47%). The subcellular localization results of the FDM versus SC group and SC versus NC group are shown in Figure S4A−D.

GO Enrichment Analysis. To elucidate the biological roles of proteins from different perspectives, we separately performed differential protein enrichment analysis from three major classes in gene ontology (GO) enrichment. Biological process (BP) analysis in the FDM versus NC group showed that most of the differential proteins were involved in blood coagulation, fibrin clot formation, plasminogen activation, regulation of wound healing, fibrinolysis, and similar BPs (Figure 3A). Molecular functional (MF) analysis revealed that differential proteins were mainly in association with the structural constituent of the eye lens, structural molecule

activity, identical protein binding, and protein homodimerization activity (Figure 3C). According to cellular composition (CC) analysis, differential proteins were mainly enriched at the extracellular space, fibrinogen complex, and supramolecular fiber (Figure 3E).

In the acetylated proteome, the analysis based on BP showed that differentially acetylated proteins were primarily engaged in nucleotide phosphorylation, nucleoside diphosphate phosphorylation, and pyridine nucleotide biosynthetic process (Figure 3B). MF analysis indicated that differentially acetylated proteins were associated primarily with unfolded protein binding, isomerase activity, and intramolecular oxidoreductase activity (Figure 3D). According to the CC analysis, differentially acetylated proteins were mainly in the myelin sheath, extracellular region, endoplasmic reticulum lumen, and photoreceptor disk membrane (Figure 3F). We additionally observed that most of the upregulated acetylated proteins were associated with the regulation of genes, while the downregulated acetylated proteins were involved in binding activity and metabolic processes. The GO enrichment analysis results of the FDM versus SC group and SC versus NC group are shown in Figures S5-1 and S5-2.

Figure 4A shows the overall output from the GO enrichment analysis of acetylated proteins, and Figure 4B−D shows acetylated proteins that were significantly changed in BP, MF, and CC, respectively. In the BP category, the significantly upregulated acetylated protein was ATP synthase peripheral stalk subunit F6 (ATP5PF), and the significantly downregulated acetylated protein was heat shock protein 90 α family class A member 1 (HSP90AA1) (Figure 4B). The chord diagram showed that hexokinase 2 (HK2), pyruvate kinase M1/2 (PKM), and hexokinase domain containing 1 (HKDC1) were involved in multiple simultaneous biological processes, including the ATP metabolic process, nucleotide phosphorylation, and positive regulation of DNA biosynthetic process. Among the MF categories, the significantly up- and downregulated acetylated proteins were peptidylprolyl isomerase like 2 (PPIL2) and atlastin GTPase 3 (ATL3), respectively (Figure 4C). In addition, the protein most highly involved in the MF was endoplasmic reticulum protein 44 (ERP44), which was involved in intramolecular oxidoreductase activity, isomerase activity, and protein disulfide isomerase activity. Nucleobindin 1 (NUCB1) was the only protein whose acetylation level was significantly downregulated in CC (Figure 4D). Moreover, G protein subunit β 1 (GNB1) and ATP binding cassette subfamily A member 4 (ABCA4) were widely present in various CC including the photoreceptor disk membrane, nonmotile cilium, and photoreceptor cell cilium.

Domain Analysis and KEGG Enrichment Analysis. Protein domains refer to components with similar sequences, structures, and functions that are present in different proteins and are units of protein evolution. There was significant enrichment of 14 protein structural domains in the domain analysis of the differential proteins, including β/γ crystallin, macroglobulin domain MG3, globin, and glutathione S-transferase C-terminal domain (Figure 5A). For differentially acetylated proteins, 18 domains were significantly enriched, including the ATP synthase α/β family, thioredoxin, thioredoxin-like domain, and hexokinase (Figure 5B).

Next, to more comprehensively characterize the biological roles of differential proteins and differentially acetylated proteins, we performed KEGG pathway enrichment analysis. In the quantitative proteome, we enriched nine pathways,
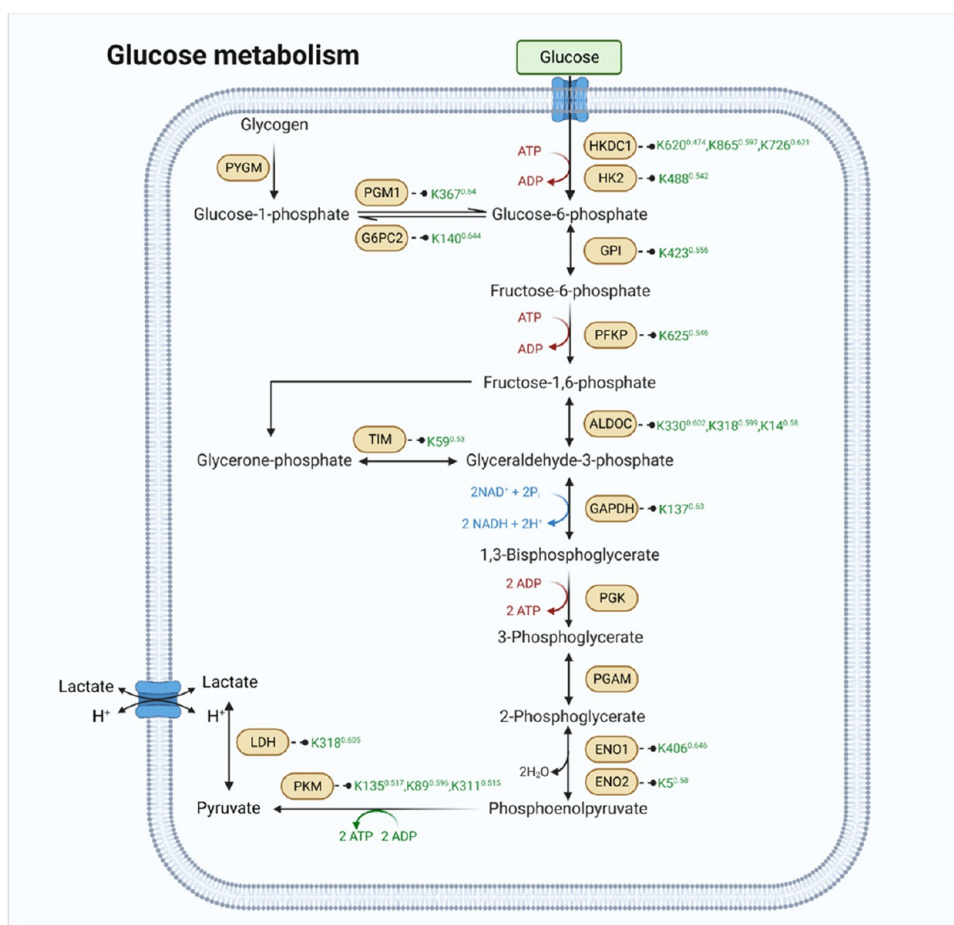
Figure 6. Map of acetylation level changes in protein sites in the retinas of the FDM and NC groups in the glucose metabolism pathway. The green numbers represented the acetylation modification sites of the enzymes and the change ratio in the FDM group versus NC group.

including complement and coagulation cascades, circadian entrainment, retinol metabolism, dopaminergic synapses, and cholinergic synapses (Figure 5C). Nevertheless, the upregulated proteins were mainly engaged in complement and coagulation cascades and retinol metabolism pathways (Table S5-1). Furthermore, differentially acetylated proteins were also mapped to the KEGG pathway, where 26 major pathways were significantly enriched (Table S5-2). The most noteworthy was the significant enrichment of differentially acetylated proteins in metabolic pathways, such as glycolysis/gluconeogenesis, fructose and mannose metabolism, galactose metabolism, and the pentose phosphate pathway, and in molecular signaling pathways regulating glucose and lipid metabolism, such as the HIF-1, PI3K/Akt, and AMPK signaling pathways (Figure 5D,E). However, there was only one significantly upregulated pathway, which was the nucleocytoplasmic transport pathway (Table S5-2). Notably, pathways that were significantly enriched in quantitative proteins showed significant downregulation in acetylation modifications, including retinol metabolism and adrenergic signaling in cardiomyocytes. Moreover, significantly downregulated pathways included those that maintain water and ion homeostasis including aldosterone-regulated sodium reabsorption and proximal tubule bicarbonate reclamation pathways, as well as signaling pathways involved in neurotransmitter transmission including glutamatergic synapse signaling, GABAergic synapse signaling, serotonergic synapse signaling, and synaptic vesicle cycle pathways.

In the acetylated proteome, Figure 5F shows that the acetylation levels of proteins were significantly altered, with the most significantly downregulated protein being ribonucleoprotein I (RPN1). HKDC1 and HK2 were involved in multiple pathways, including the HIF-1 signaling pathway, glycolysis/gluconeogenesis, starch and sucrose metabolism, and fructose and mannose metabolism. To investigate whether Kac can be involved in the progression of FDM by affecting retinal metabolism, we further analyzed the glucose metabolic pathway, in which 13 differentially acetylated proteins between FDM and NC exhibited 19 downregulated Kac sites (Figure 6). The results of the protein domain and KEGG pathway enrichment analysis for the FDM versus SC group and SC versus NC group are presented in Figures S6-1 and S6-2.

PPI Networks. To further explore how acetylation regulates metabolic processes in the retina in response to the stress of form deprivation, we constructed a PPI network for differentially acetylated proteins (Figure 7A). In total, the MCODE mapped 212 differentially acetylated proteins and showed the top three most compact MCODE modules: MCODE 1 (score = 12.138) was made of 30 nodes and 176 edges (Figure 7B), MCODE 2 (score = 7.467) was made of 16 nodes and 56 edges (Figure 7C), and MCODE 3 (score = 6.889) was made of 28 nodes and 93 edges (Figure 7D). Moreover, CytoHubba has selected the top 10 hub proteins in the PPI network, which were highlighted in the table with a dark blue background (Table S6). In addition, we found that the proteins in MCODE 1 were mainly related to ribosomes
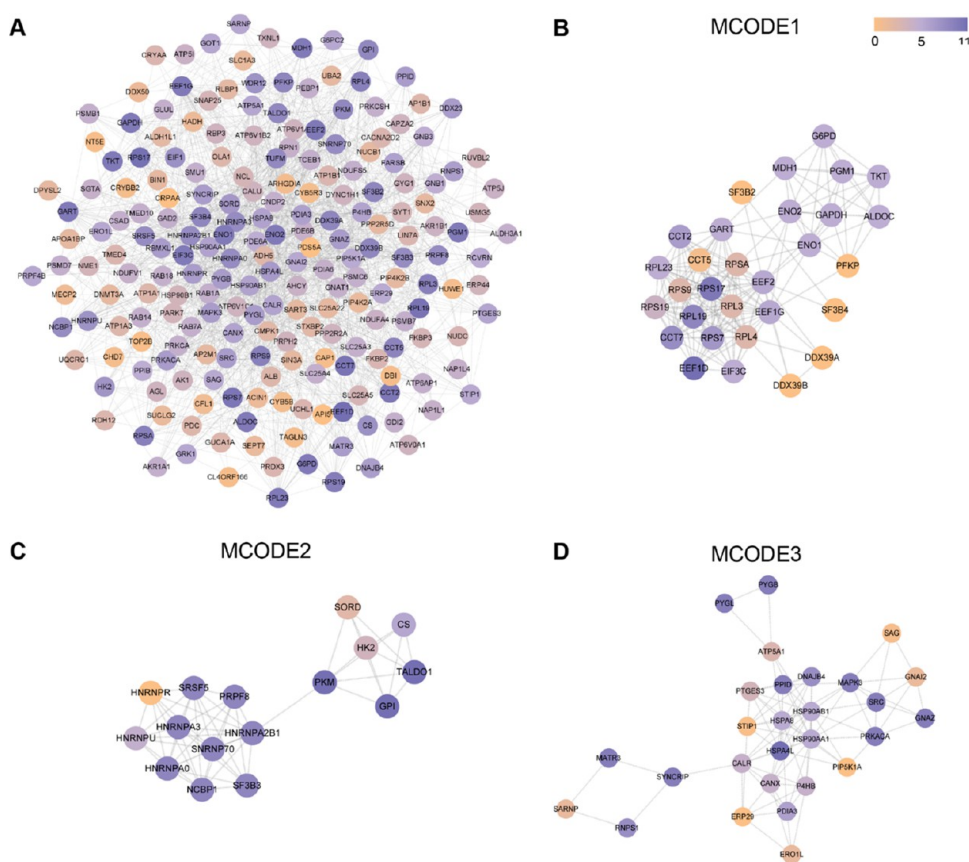
Figure 7. PPI network analysis of differentially acetylated proteins. (A) PPI network of total differentially acetylated proteins identified in the database. (B) MCODE 1 in the acetylated proteomic network. (C) MCODE 2 in the acetylated proteomic network. (D) MCODE 3 in the acetylated proteomic network.

and glycolysis/gluconeogenesis, those in MCODE 2 were mostly related to proteins in the spliceosome, and those in MCODE 3 were associated with protein processing in the endoplasmic reticulum. The complex interactions between acetylated proteins indicated their potential to interoperate during form deprivation.

Distribution and Motif Analysis of Lysine Acetylation Sites. Figure 8A shows the distribution of modification sites in acetylated proteins. The results indicated that the percentage of proteins containing one, two, and three acetylation sites was 82.94% (355/428), 10.28% (44/428), and 3.74% (16/428), respectively. Next, to further characterize the acetylation sites, the aa motifs surrounding the modification sites (10 aa up- and downstream of the Kac sites) were analyzed using the motif-x algorithm. The 5329 detected peptides matched a total of 29 conserved motifs, and the top 10 motifs were displayed based on motif scores (Figure 8B and Table S7). The first 10 motifs included G-1K^{ac}L+1, V-1K^{ac}R+1, G-1K^{ac}I+2, A-1K^{ac}L+1, S-1K^{ac}L+1, H-2K^{ac}L+1, D-1K^{ac}D+1, Y-3K^{ac}V+1, K^{ac}L+1, and K^{ac}I+1. Enrichment of glycine (G), valine (V), alanine (A), serine (S), histidine (H), aspartic acid (D), and tyrosine (Y) residues were found upstream of the acetylated lysine, whereas leucine (L), arginine (R), isoleucine (I), D, and V residues were found downstream of the Kac sites. The enrichment of most of the conserved residues near the Kac site (e.g., C, E, and P) was significantly reduced depending on the position of these residues. However, residues F, G, H, and V strongly favored position ±1 or ±2 (Figure 8C). We thus speculated

that proteins with these motifs would be more readily recognized by lysine acetyltransferases.

■ DISCUSSION

The present study showed a refractive shift of 5.13 ± 0.50 D and an axial shift of 0.36 ± 0.05 mm at 2 postoperative weeks in the FDM group. However, a previous study showed that 2 weeks of form deprivation induced a myopic shift of 2.21 ± 2.11 D.[24] It seemed that the extent of myopia was greater here, probably because the form deprivation was applied on 3-week-old guinea pigs in previous studies, whereas we used 2-week-old guinea pigs whose development of refractive error was more sensitive to visual distortion. In addition, since the form-deprivation hood we used was modified from the latex balloon made by Lu et al., perhaps the lower light transmission of our hood caused a greater blurring of the retinal image.

Notably, a trend toward axial elongation was also observed in eyes contralateral to form deprivation (SC group), but no significant difference was observed in refraction or AL compared to normal control eyes. Similarly, previous studies have found that form deprivation to one eye would affect the refractive and axial development of the contralateral eye in animal models including macaques,[27] tree rats,[28] chickens,[29] and mice.[30] However, there was no explanation from the authors as to why the contralateral eye tended to change similarly to the form-deprived eye, even though the contralateral eye did not develop myopia. Yang et al. similarly noted this phenomenon and found that some similar metabolic changes were observed in the retina of the uncovered
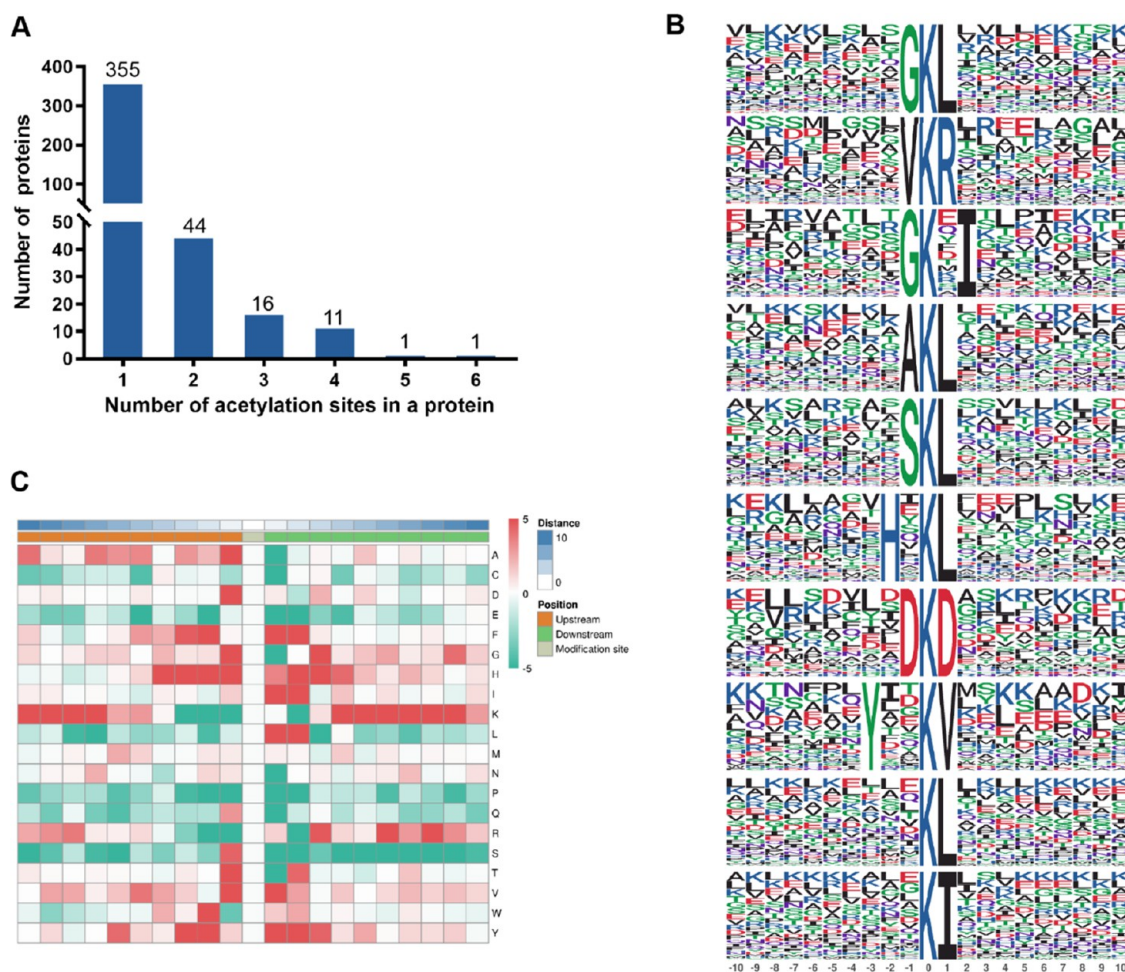
Figure 8. Bioinformatic profiling of the Kac sites. (A) Distribution of the number of Kac sites in acetylated proteins. (B) Top 10 conserved motifs. (C) Heatmap of the aa near the Kac site according to the frequency of occurrence.

contralateral eye, albeit at increased or decreased levels compared to those in corresponding form-deprived eye.[31] This is similar to the parallel reduction of lysine acetylation modification levels in form-deprived and self-control eyes in the present study (Figure 1E), but the reduction in acetylation modification levels in self-control eyes was smaller than in form-deprived eyes, which may explain the discrepancy. We can explain the decrease in the level of Kac modification by affecting the metabolic regulatory process,[32] which leads to disruption of retinal metabolism and thus initiates the retina—choroid—sclera signaling cascade pathway in myopia.[33]

In this study, a 4D label-free quantitative method was used to perform quantitative proteomic analysis on the retinas of form-deprived myopic guinea pigs.[34] We identified a total of 6568 differential proteins, of which 48 proteins were upregulated and 37 proteins were downregulated in the FDM compared to the NC group. In the KEGG pathway enrichment analysis, the significantly upregulated pathways were the complement and coagulation cascades and the retinol metabolic pathway. Riddell et al. examined gene expression in experimentally myopic chicks using RNA sequencing and meta-analysis successively and found transcriptional activation associated with the immune and complement systems.[35,36] Giummarra et al. suggested that significant upregulation of the complement and coagulation cascade pathways during the induction of form-deprivation myopia may be related to

physiological stress mechanisms associated with choroidal contraction and reduced blood flow.[37] Subsequently, García-Gen et al. demonstrated the correlation between the level of complement factor H (CFH) in aqueous humor and myopic choroidal atrophy in patients with high myopia.[38] Thus, our results confirm the activation of the complement system in the myopic retina at the protein level, which may be associated with decreased choroidal blood flow and atrophy in myopic eyes; however, additional molecular and cellular experiments are needed to confirm this finding.

Second, we found that the retinol metabolic pathway was upregulated in the quantitative proteome, while the enzymes involved in the retinoic acid synthesis and metabolism pathway were downregulated in the lysine-acetylated proteome. In this pathway, all-trans-retinol (vitamin A) was synthesized to all-trans-retinal by alcohol dehydrogenases (ADHs) or retinol dehydrogenases (RDHs) and subsequently oxidized to all-trans retinoic acid (atRA) by cytoplasmic retinaldehyde dehydrogenase (RALDH1/2/3). Then, atRA bound to the dimer of the RA receptor (RAR) and retinoid-X receptor (RXR), followed by binding to DNA and affecting transcription.[39] Increased retinal atRA after FDM has been shown in guinea pigs[40] and chicken.[41] The retinal pigment epithelium 65 kDa protein (RPE65) was a significantly upregulated protein in the quantitative proteome in this study, and we suggested that it may be involved in the development of FDM through its

participation in the retinol metabolic pathway. It has been shown that the interaction of RPE65 with RDH5 was important for the efficient transfer of retinoids and the adequate and rapid production of retinal.[42] Thus, upregulation of RPE65 in the FDM retina may contribute to retinol synthesis, which leads to increased atRA synthesis. Additionally, there were significant downregulation of the acetylation levels of RDH and ADH in this study. The possible mechanism could be due to the increased RA level in the retina during the development of FDM, which negatively feedback regulated the acetylation levels of RDH and ADH.[43]

Subsequently, a quantitative analysis of the acetylated proteome in the FDM retina was performed to explore the pathogenesis of the post-translational protein modification levels. In the current study, we identified a total of 2318 acetylated proteins and 5677 Kac sites. There were 17 upregulated acetylated proteins and 297 downregulated acetylated proteins identified in the FDM group versus NC group. Based on subcellular localization analysis, it was found that both quantitative proteome and acetylated proteome differentially expressed proteins that were significantly altered dominated the cytoplasm. This discovery was reasonable given that the cytoplasm contains enzymes catalyzing various biochemical reactions and was known to be the primary cellular activity site. This should not be surprising, as the biochemical and metabolic activity in the retina is dynamic. The results of this study revealed that differentially acetylated proteins were significantly enriched in various metabolic pathways including glycolysis/gluconeogenesis, galactose metabolism, and pentose phosphate pathway, indicating that acetylation modifications contribute to the regulation of metabolic abnormalities in FDM, which may offer new perspectives on the mechanism underlying FDM.

Notably, the levels of protein acetylation of HK2 and HKDC1 were significantly reduced and were involved in various metabolic pathways, such as the HIF-1 signaling pathway, glycolysis/glycogenesis, and starch and sucrose metabolism. Hexokinases (HKs) are key enzymes that catalyze the first step of metabolizing glucose into glucose-6-phosphate during glycolysis. There are four isomers of HKs in mammals including HK1-4.[44] Hexokinase 2 (HK2) is one of the main regulators of aerobic glycolysis.[45] The HK2 was most intensely expressed in the inner segments of photoreceptors as well as in the perinuclear region (especially in the retinal cone cells) in both mouse and rat retinas.[46,47] Weh showed that HK2 was essential for maintaining photoreceptors during acute nutritional stress and aging.[45] HKDC1 is a novel hexokinase gene homologous to HK1-4 in the family of hexokinase genes participating in the glucose metabolism.[48] The reduced acetylation of GAPDH, PKM, LDH, and ENO1 examined in the FDM retina may imply the reduction in the catalytic activity of these enzymes and an impaired glycolytic function. The mammalian retina is one of the tissues that primarily undergoes aerobic glycolysis, converting most of the glucose to lactate instead of its complete breakdown to carbon dioxide by oxidative phosphorylation, even though there are fully functional mitochondria and an adequate oxygen supply.[49,50] Multiple studies have demonstrated the impact of inhibiting glycolysis on retinal function and survival. Ames et al. found that the absence of glucose in the cell medium resulted in a rapid decrease in the electrical response of the rabbit retina in *vitro*, confirming the importance of aerobic glycolysis for retinal function.[51] Similarly, Winkler et al. found that glucose

deprivation in the rat retina or treatment with glycolysis inhibitors resulted in a loss of fast PIII wave amplitude.[49] It was shown by Chertov et al. that glycolysis is required for photoreceptor survival in mouse explants and that alternative mitochondrial fuel availability would delay but not stop the increase of cell death induced by glucose deprivation.[52] However, the connection between glycolysis and myopia has been reported before in the retina of myopic mice and the sclera of myopic or recovering tree shrews.[53,54] Yang et al. also reported that the development of myopia was linked to decrease tricarboxylic acid cycle turnover and impaired glucose cycling.[31] Collectively, we found for the first time that the Kac levels of HK2, HKDC1, PKM, LDH, GAPDH, and ENO1, key regulatory enzymes in the glycolysis pathway, were significantly downregulated in the retinas of FDM guinea pigs. Integrating previous studies and our acetylated proteome study, we hypothesized that Kac alterations in these proteins might influence the function of retinal photoreceptors through the glycolysis pathway. However, the fundamental mechanisms underlying the different acetylation sites of these enzymes in regulating enzymatic activity and thus affecting glucose metabolism in retinal cells needed to be further investigated.

Data from KEGG pathway enrichment analysis revealed that the differentially acetylated proteins identified in this study were in multiple molecular signaling pathways that regulate glucose and lipid metabolism, including the HIF-1, PI3K-Akt, and AMPK signaling pathways. It has been shown that key enzymes related to glucose and lipid metabolism, such as HK2, PKM, LDH, GAPDH, and phosphofructokinase platelets (PFKP) were regulated by the above signaling pathways.[55] In addition, pathways that maintain water and ion homeostasis were significantly downregulated, including aldosterone-regulated sodium reabsorption and proximal tubular bicarbonate recycling pathways. In particular, proteins with significantly downregulated levels of Kac included the ATPase Na^+/K^+ transport subunits $\alpha1/\alpha3/\beta1$ (ATP1A1/ATP1A3/ATP1B1). All three proteins above belong to the Na^+/K^+-ATPase subfamily, and Na^+/K^+-ATPase was a complete membrane protein which established and maintained the electrochemical gradient of Na^+ and K^+ crossing the plasma membrane.[56] Liang et al.[57] and Crewther et al.[58] also used scanning electron microscopy and elemental microanalysis to prove that Na^+ and K^+ concentrations in the ocular posterior pole increased after form deprivation. In brief, our results suggested that Kac may play a role in the regulation of water and ion homeostasis, thereby affecting FDM formation. Moreover, some enzymes involved in neurotransmitter signaling pathways also showed downregulation of acetylation levels, such as glutamate ammonia ligase (GLUL) in glutamatergic synapses and glutamate decarboxylase 2 (GAD2) in GABAergic synapses. Glutamate and γ-aminobutyric acid (GABA) are the major excitatory and inhibitory neurotransmitters in the vertebrate retina, and they play an important role in visual information processing.[59] It has been found that an imbalance in the ratio between GABA and glutamate was considered one of the signals for myopia triggers.[9] According to drug studies, the GABAB receptor antagonist CGP46381 could attenuate the progression of FDM in guinea pigs.[60] Hence, deacetylation of lysine residues in GAD2 and GLUL might influence their enzymatic activity and thus the associated catalytic reaction, which might be related to changes in glutamate and GABA contents.

CONCLUSIONS

Generally, advanced studies of the relationships between acetylation levels and the catalytic reactions of enzymes of important proteins are necessary. Although the results of this study revealed that the acetylation levels of many proteins are downregulated under form-deprivation conditions, some limitations of our study need to be considered. First, we performed experiments on guinea pig retinas after only 2 weeks of form deprivation and did not test acetylation levels at other time points. Next, some key low-abundance proteins might have been missed due to the sensitivity of the mass spectrometry technique and the threshold limit used for differential analysis. In addition, alterations in acetylation modifications of key enzymes in the form-deprived retina might affect their activity. However, the molecular mechanism by which Kac regulates retinal energy metabolism has not been elucidated. Therefore, our results require additional experimental verification. In summary, Kac plays a key role in metabolic regulation in FDM, and the results of this study provide a new perspective to elucidate the pathogenesis of myopia.

ASSOCIATED CONTENT

Ⓢ Supporting Information

The Supporting Information is available free of charge at https://pubs.acs.org/doi/10.1021/acsomega.3c02219.

> Figure S1: PCA for the quantitative proteome and acetylated proteome; Figure S2: distribution of peptide length for the quantitative proteome and acetylated proteome; Figure S3: heatmap for differential proteins and differentially acetylated proteins; Figure S4: rose plot of the subcellular localization of differentially expressed proteins in the FDM group versus SC group and SC group versus the NC group in the quantitative proteome and the acetylated proteome; Figure S5-1: bar graph of GO enrichment analysis of the FDM versus SC group in the quantitative proteome and acetylated proteome; Figure S5-2: bar graph of GO enrichment analysis of the SC versus NC group in the quantitative proteome and acetylated proteome; Figure S6-1: protein domain and KEGG pathway enrichment analysis of quantitative proteome and acetylated proteome for the FDM group versus SC group; and Figure S6-2: protein domain and KEGG pathway enrichment analysis of the quantitative proteome and the acetylated proteome for the SC group versus NC group (PDF)

> Table S1: detailed information of all quantified proteins; Table S2: identified lysine-acetylated protein information; Table S3: detailed information on differential proteins; Table S4: detailed information on differentially acetylated proteins; Table S5-1: KEGG pathway analysis of the quantitative proteome; Table S5-2: KEGG pathway analysis of the acetylated proteins; Table S6: information on protein interaction networks; and Table S7: motif retrieved from lysine-acetylated peptides (ZIP)

AUTHOR INFORMATION

Corresponding Authors

Jike Song − Shandong University of Traditional Chinese Medicine, Jinan 250014 Shandong, China; Affiliated Eye Hospital of Shandong University of Traditional Chinese Medicine, Jinan 250002 Shandong, China; Email: edusjk@163.com

Hongsheng Bi − Affiliated Eye Hospital of Shandong University of Traditional Chinese Medicine, Jinan 250002 Shandong, China; Shandong Provincial Key Laboratory of Integrated Traditional Chinese and Western Medicine for Prevention and Therapy of Ocular Diseases, Shandong Academy of Eye Disease Prevention and Therapy, Jinan 250002 Shandong, China; Email: hongshengbi1@163.com

Authors

Jiaojiao Feng − Shandong University of Traditional Chinese Medicine, Jinan 250014 Shandong, China; ⓘ orcid.org/0000-0002-3286-7982

Xiuyan Zhang − Affiliated Eye Hospital of Shandong University of Traditional Chinese Medicine, Jinan 250002 Shandong, China; Shandong Provincial Key Laboratory of Integrated Traditional Chinese and Western Medicine for Prevention and Therapy of Ocular Diseases, Shandong Academy of Eye Disease Prevention and Therapy, Jinan 250002 Shandong, China

Runkuan Li − Shandong University of Traditional Chinese Medicine, Jinan 250014 Shandong, China

Ping Zhao − Affiliated Eye Hospital of Shandong University of Traditional Chinese Medicine, Jinan 250002 Shandong, China; Shandong Provincial Key Laboratory of Integrated Traditional Chinese and Western Medicine for Prevention and Therapy of Ocular Diseases, Shandong Academy of Eye Disease Prevention and Therapy, Jinan 250002 Shandong, China

Xudong Han − School of Medicine, Southeast University, Nanjing 210009 Jiangsu, China

Qiuxin Wu − Affiliated Eye Hospital of Shandong University of Traditional Chinese Medicine, Jinan 250002 Shandong, China; Shandong Provincial Key Laboratory of Integrated Traditional Chinese and Western Medicine for Prevention and Therapy of Ocular Diseases, Shandong Academy of Eye Disease Prevention and Therapy, Jinan 250002 Shandong, China

Qingmei Tian − Affiliated Eye Hospital of Shandong University of Traditional Chinese Medicine, Jinan 250002 Shandong, China; Shandong Provincial Key Laboratory of Integrated Traditional Chinese and Western Medicine for Prevention and Therapy of Ocular Diseases, Shandong Academy of Eye Disease Prevention and Therapy, Jinan 250002 Shandong, China

Guodong Tang − Affiliated Eye Hospital of Shandong University of Traditional Chinese Medicine, Jinan 250002 Shandong, China; Shandong Provincial Key Laboratory of Integrated Traditional Chinese and Western Medicine for Prevention and Therapy of Ocular Diseases, Shandong Academy of Eye Disease Prevention and Therapy, Jinan 250002 Shandong, China

Complete contact information is available at:
https://pubs.acs.org/10.1021/acsomega.3c02219

Author Contributions

J.F., X.Z., and R.L. performed the experiments. J.F. analyzed and wrote the manuscript. J.S. revised the manuscript and conceived and supervised the study. All authors have approved the final version of the manuscript.

Notes

The authors declare the following competing financial interest(s): The mass spectrometry proteomics data of the proteome and acetylated proteome have been deposited into the ProteomeXchange consortium via the PRIDE partner repository with the dataset identifier PXD043226 and PXD043196.

■ ABBREVIATIONS

FDM, form-deprivation myopia; Kac, lysine acetylation; PTMs, post-translational modifications; HK2, hexokinase 2; HKDC1, hexokinase domain containing 1; PKM, pyruvate kinase M1/2

■ REFERENCES

(1) Jong, M.; Jonas, J. B.; Wolffsohn, J. S.; Berntsen, D. A.; Cho, P.; Clarkson-Townsend, D.; Flitcroft, D. I.; Gifford, K. L.; Haarman, A. E. G.; Pardue, M. T.; Richdale, K.; Sankaridurg, P.; Tedja, M. S.; Wildsoet, C. F.; Bailey-Wilson, J. E.; Guggenheim, J. A.; Hammond, C. J.; Kaprio, J.; MacGregor, S.; Mackey, D. A.; Musolf, A. M.; Klaver, C. C. W.; Verhoeven, V. J. M.; Vitart, V.; Smith, E. L. IMI 2021 Yearly Digest. *Invest. Ophthalmol. Vis. Sci.* **2021**, *62*, 7.

(2) Hudson, D. M.; Joeng, K. S.; Werther, R.; Rajagopal, A.; Weis, M.; Lee, B. H.; Eyre, D. R. Post-Translationally Abnormal Collagens of Prolyl 3-Hydroxylase-2 Null Mice Offer a Pathobiological Mechanism for the High Myopia Linked to Human LEPREL1 Mutations. *J. Biol. Chem.* **2015**, *290*, 8613−8622.

(3) Holden, B. A.; Fricke, T. R.; Wilson, D. A.; Jong, M.; Naidoo, K. S.; Sankaridurg, P.; Wong, T. Y.; Naduvilath, T. J.; Resnikoff, S. Global Prevalence of Myopia and High Myopia and Temporal Trends from 2000 through 2050. *Ophthalmology* **2016**, *123*, 1036−1042.

(4) Ohno-Matsui, K.; Lai, T. Y. Y.; Lai, C.-C.; Cheung, C. M. G. Updates of Pathologic Myopia. *Prog. Retinal Eye Res.* **2016**, *52*, 156−187.

(5) Ruiz-Medrano, J.; Montero, J. A.; Flores-Moreno, I.; Arias, L.; García-Layana, A.; Ruiz-Moreno, J. M. Myopic Maculopathy: Current Status and Proposal for a New Classification and Grading System (ATN). *Prog. Retinal Eye Res.* **2019**, *69*, 80−115.

(6) Brown, D. M.; Mazade, R.; Clarkson-Townsend, D.; Hogan, K.; Datta Roy, P. M.; Pardue, M. T. Candidate Pathways for Retina to Scleral Signaling in Refractive Eye Growth. *Exp. Eye Res.* **2022**, *219*, No. 109071.

(7) Chakraborty, R.; Ostrin, L. A.; Benavente-Perez, A.; Verkicharla, P. K. Optical Mechanisms Regulating Emmetropisation and Refractive Errors: Evidence from Animal Models. *Clin. Exp. Optom.* **2020**, *103*, 55−67.

(8) Troilo, D.; Smith, E. L.; Nickla, D. L.; Ashby, R.; Tkatchenko, A. V.; Ostrin, L. A.; Gawne, T. J.; Pardue, M. T.; Summers, J. A.; Kee, C.-S.; Schroedl, F.; Wahl, S.; Jones, L. IMI - Report on Experimental Models of Emmetropization and Myopia. *Invest. Ophthalmol. Vis. Sci.* **2019**, *60*, M31−M88.

(9) Guoping, L.; Xiang, Y.; Jianfeng, W.; Dadong, G.; Jie, H.; Wenjun, J.; Junguo, G.; Hongsheng, B. Alterations of Glutamate and γ-Aminobutyric Acid Expressions in Normal and Myopic Eye Development in Guinea Pigs. *Invest. Ophthalmol. Vis. Sci.* **2017**, *58*, 1256.

(10) Liu, S.; Chen, H.; Ma, W.; Zhong, Y.; Liang, Y.; Gu, L.; Lu, X.; Li, J. Non-coding RNAs and Related Molecules Associated with Form-deprivation Myopia in Mice. *J. Cell. Mol. Med.* **2022**, *26*, 186−194.

(11) Pan, F. Defocused Image Changes Signaling of Ganglion Cells in the Mouse Retina. *Cells* **2019**, *8*, 640.

(12) Bian, J.; Sze, Y.-H.; Tse, D. Y.-Y.; To, C.-H.; McFadden, S. A.; Lam, C. S.-Y.; Li, K.-K.; Lam, T. C. SWATH Based Quantitative Proteomics Reveals Significant Lipid Metabolism in Early Myopic Guinea Pig Retina. *Int. J. Mol. Sci.* **2021**, *22*, 4721.

(13) Yu, F.-J.; Lam, T. C.; Sze, A. Y.-H.; Li, K.-K.; Chun, R. K.-M.; Shan, S.-W.; To, C.-H. Alteration of Retinal Metabolism and Oxidative Stress May Implicate Myopic Eye Growth: Evidence from Discovery and Targeted Proteomics in an Animal Model. *J. Proteomics* **2020**, *221*, No. 103684.

(14) Yu, F.-j.; Lam, T.; Liu, L.; Chun, R. K.; Cheung, J. K.; Li, K.; To, C. Isotope-Coded Protein Label Based Quantitative Proteomic Analysis Reveals Significant up-Regulation of Apolipoprotein A1 and Ovotransferrin in the Myopic Chick Vitreous. *Sci. Rep.* **2017**, *7*, No. 12649.

(15) Zhu, Y.; Bian, J. F.; Lu, D. Q.; To, C. H.; Lam, C. S.-Y.; Li, K. K.; Yu, F. J.; Gong, B. T.; Wang, Q.; Ji, X. W.; Zhang, H. M.; Nian, H.; Lam, T. C.; Wei, R. H. Alteration of EIF2 Signaling, Glycolysis, and Dopamine Secretion in Form-Deprived Myopia in Response to 1% Atropine Treatment: Evidence From Interactive ITRAQ-MS and SWATH-MS Proteomics Using a Guinea Pig Model. *Front. Pharmacol.* **2022**, *13*, No. 814814.

(16) Stram, A. R.; Payne, R. M. Posttranslational Modifications in Mitochondria: Protein Signaling in the Powerhouse. *Cell. Mol. Life Sci.* **2016**, *73*, 4063−4073.

(17) Shvedunova, M.; Akhtar, A. Modulation of Cellular Processes by Histone and Non-Histone Protein Acetylation. *Nat. Rev. Mol. Cell Biol.* **2022**, *23*, 329−349.

(18) Allfrey, V. G.; Faulkner, R.; Mirsky, A. E. Acetylation And Methylation Of Histones And Their Possible Role In The Regulation Of RNA Synthesis. *Proc. Natl. Acad. Sci. U.S.A.* **1964**, *51*, 786−794.

(19) Weinert, B. T.; Wagner, S. A.; Horn, H.; Henriksen, P.; Liu, W. R.; Olsen, J. V.; Jensen, L. J.; Choudhary, C. Proteome-Wide Mapping of the *Drosophila* Acetylome Demonstrates a High Degree of Conservation of Lysine Acetylation. *Sci. Signal.* **2011**, *4*, ra48.

(20) Baeza, J.; Smallegan, M. J.; Denu, J. M. Mechanisms and Dynamics of Protein Acetylation in Mitochondria. *Trends Biochem. Sci.* **2016**, *41*, 231−244.

(21) Zhao, S.; Xu, W.; Jiang, W.; Yu, W.; Lin, Y.; Zhang, T.; Yao, J.; Zhou, L.; Zeng, Y.; Li, H.; Li, Y.; Shi, J.; An, W.; Hancock, S. M.; He, F.; Qin, L.; Chin, J.; Yang, P.; Chen, X.; Lei, Q.; Xiong, Y.; Guan, K.-L. Regulation of Cellular Metabolism by Protein Lysine Acetylation. *Science* **2010**, *327*, 1000−1004.

(22) Wang, Y.-P.; Zhou, L.-S.; Zhao, Y.-Z.; Wang, S.-W.; Chen, L.-L.; Liu, L.-X.; Ling, Z.-Q.; Hu, F.-J.; Sun, Y.-P.; Zhang, J.-Y.; Yang, C.; Yang, Y.; Xiong, Y.; Guan, K.-L.; Ye, D. Regulation of G6PD Acetylation by SIRT2 and KAT9 Modulates NADPH Homeostasis and Cell Survival during Oxidative Stress. *EMBO J.* **2014**, *33*, 1304−1320.

(23) Pehar, M.; Ball, L. E.; Sharma, D. R.; Harlan, B. A.; Comte-Walters, S.; Neely, B. A.; Vargas, M. R. Changes in Protein Expression and Lysine Acetylation Induced by Decreased Glutathione Levels in Astrocytes. *Mol. Cell. Proteomics* **2016**, *15*, 493−505.

(24) Lu, F.; Zhou, X.; Zhao, H.; Wang, R.; Jia, D.; Jiang, L.; Xie, R.; Qu, J. Axial Myopia Induced by a Monocularly-Deprived Facemask in Guinea Pigs: A Non-Invasive and Effective Model. *Exp. Eye Res.* **2006**, *82*, 628−636.

(25) Wan, J.; Hu, M.; Jiang, Z.; Liu, D.; Pan, S.; Zhou, S.; Liu, Z. Lysine Acetylation in the Proteome of Renal Tubular Epithelial Cells in Diabetic Nephropathy. *Front. Genet.* **2021**, *12*, No. 767135.

(26) Li, Y.; Xue, H.; Bian, D.; Xu, G.; Piao, C. Acetylome Analysis of Lysine Acetylation in the Plant Pathogenic Bacterium Brenneria Nigrifluens. *MicrobiologyOpen* 2019, 9, No. e00952.

(27) Bradley, D. V.; Fernandes, A.; Boothe, R. G. The Refractive Development of Untreated Eyes of Rhesus Monkeys Varies According to the Treatment Received by Their Fellow Eyes. *Vision Res.* 1999, 39, 1749−1757.

(28) McBrien, N. A.; Norton, T. T. The Development of Experimental Myopia and Ocular Component Dimensions in Monocularly Lid-Sutured Tree Shrews (*Tupaia Belangeri*). *Vision Res.* 1992, 32, 843−852.

(29) Wildsoet, C.; Wallman, J. Choroidal and Scleral Mechanisms of Compensation for Spectacle Lenses in Chicks. *Vision Res.* 1995, 35, 1175−1194.

(30) Schaeffel, F.; Burkhardt, E.; Howland, H. C.; Williams, R. W. Measurement of Refractive State and Deprivation Myopia in Two Strains of Mice. *Optom. Vis. Sci.* 2004, 81, 99−110.

(31) Yang, J.; Reinach, P. S.; Zhang, S.; Pan, M.; Sun, W.; Liu, B.; Li, F.; Li, X.; Zhao, A.; Chen, T.; Jia, W.; Qu, J.; Zhou, X. Changes in Retinal Metabolic Profiles Associated with Form Deprivation Myopia Development in Guinea Pigs. *Sci. Rep.* 2017, 7, No. 2777.

(32) Overmyer, K. A.; Evans, C. R.; Qi, N. R.; Minogue, C. E.; Carson, J. J.; Chermside-Scabbo, C. J.; Koch, L. G.; Britton, S. L.; Pagliarini, D. J.; Coon, J. J.; Burant, C. F. Maximal Oxidative Capacity during Exercise Is Associated with Skeletal Muscle Fuel Selection and Dynamic Changes in Mitochondrial Protein Acetylation. *Cell Metab.* 2015, 21, 468−478.

(33) Huang, Y.; Chen, X.; Zhuang, J.; Yu, K. The Role of Retinal Dysfunction in Myopia Development. *Cell. Mol. Neurobiol.* 2022, 10, 1007.

(34) Meier, F.; Brunner, A.-D.; Koch, S.; Koch, H.; Lubeck, M.; Krause, M.; Goedecke, N.; Decker, J.; Kosinski, T.; Park, M. A.; Bache, N.; Hoerning, O.; Cox, J.; Räther, O.; Mann, M. Online Parallel Accumulation−Serial Fragmentation (PASEF) with a Novel Trapped Ion Mobility Mass Spectrometer. *Mol. Cell. Proteomics* 2018, 17, 2534−2545.

(35) Riddell, N.; Giummarra, L.; Hall, N. E.; Crewther, S. G. Bidirectional Expression of Metabolic, Structural, and Immune Pathways in Early Myopia and Hyperopia. *Front. Neurosci.* 2016, 10, 390.

(36) Riddell, N.; Crewther, S. G. Novel Evidence for Complement System Activation in Chick Myopia and Hyperopia Models: A Meta-Analysis of Transcriptome Datasets. *Sci. Rep.* 2017, 7, No. 9719.

(37) Giummarra, L.; Crewther, S. G.; Riddell, N.; Murphy, M. J.; Crewther, D. P. Pathway Analysis Identifies Altered Mitochondrial Metabolism, Neurotransmission, Structural Pathways and Comple-ment Cascade in Retina/RPE/ Choroid in Chick Model of Form-Deprivation Myopia. *PeerJ* 2018, 6, No. e5048.

(38) García-Gen, E.; Penadés, M.; Mérida, S.; Desco, C.; Araujo-Miranda, R.; Navea, A.; Bosch-Morell, F. High Myopia and the Complement System: Factor H in Myopic Maculopathy. *J. Clin. Med.* 2021, 10, 2600.

(39) Pollock, L. M.; Xie, J.; Bell, B. A.; Anand-Apte, B. Retinoic Acid Signaling Is Essential for Maintenance of the Blood-Retinal Barrier. *FASEB J.* 2018, 32, 5674−5684.

(40) McFadden, S. A.; Howlett, M. H. C.; Mertz, J. R. Retinoic Acid Signals the Direction of Ocular Elongation in the Guinea Pig Eye. *Vision Res.* 2004, 44, 643−653.

(41) Seko, Y.; Shimizu, M.; Tokoro, T. Retinoic Acid Increases in the Retina of the Chick with Form Deprivation Myopia. *Ophthalmic Res.* 1998, 30, 361−367.

(42) Kiser, P. D. Retinal Pigment Epithelium 65 KDa Protein (RPE65): An Update. *Prog. Retinal Eye Res.* 2022, 88, No. 101013.

(43) Kedishvili, N. Y. Retinoic Acid Synthesis and Degradation. *Subcell. Biochem.* 2016, 81, 127.

(44) Roberts, D. J.; Miyamoto, S. Hexokinase II Integrates Energy Metabolism and Cellular Protection: Akting on Mitochondria and TORCing to Autophagy. *Cell Death Differ.* 2015, 22, 248−257.

(45) Weh, E.; Lutrzykowska, Z.; Smith, A.; Hager, H.; Pawar, M.; Wubben, T. J.; Besirli, C. G. Hexokinase 2 Is Dispensable for Photoreceptor Development but Is Required for Survival during Aging and Outer Retinal Stress. *Cell Death Dis.* 2020, 11, 422.

(46) Petit, L.; Ma, S.; Cipi, J.; Cheng, S.-Y.; Zieger, M.; Hay, N.; Punzo, C. Aerobic Glycolysis Is Essential for Normal Rod Function and Controls Secondary Cone Death in Retinitis Pigmentosa. *Cell Rep.* 2018, 23, 2629−2642.

(47) Rueda, E. M.; Johnson, J. E.; Giddabasappa, A.; Swaroop, A.; Brooks, M. J.; Sigel, I.; Chaney, S. Y.; Fox, D. A. The Cellular and Compartmental Profile of Mouse Retinal Glycolysis, Tricarboxylic Acid Cycle, Oxidative Phosphorylation, and ∼P Transferring Kinases. *Mol. Vis.* 2016, 22, 847−885.

(48) Saleheen, D.; Natarajan, P.; Armean, I. M.; Zhao, W.; Rasheed, A.; Khetarpal, S.; Won, H.-H.; Karczewski, K. J.; O'Donnell-Luria, A. H.; Samocha, K. E.; Weisburd, B.; Gupta, N.; Zaidi, M.; Samuel, M.; Imran, A.; Abbas, S.; Majeed, F.; Ishaq, M.; Akhtar, S.; Trindade, K.; Mucksavage, M.; Qamar, N.; Zaman, K. S.; Yaqoob, Z.; Saghir, T.; Rizvi, S. N. H.; Memon, A.; Mallick, N. H.; Ishaq, M.; Rasheed, S. Z.; Memon, F.-R.; Mahmood, K.; Ahmed, N.; Do, R.; Krauss, R. M.; MacArthur, D. G.; Gabriel, S.; Lander, E. S.; Daly, M. J.; Frossard, P.; Danesh, J.; Rader, D. J.; Kathiresan, S. Human Knockouts and Phenotypic Analysis in a Cohort with a High Rate of Consanguinity. *Nature* 2017, 544, 235−239.

(49) Winkler, B. S. Glycolytic and Oxidative Metabolism in Relation to Retinal Function. *J. Gen. Physiol.* 1981, 77, 667−692.

(50) Ng, S. K.; Wood, J. P.; Chidlow, G.; Han, G.; Kittipassorn, T.; Peet, D. J.; Casson, R. J. Cancer-like Metabolism of the Mammalian Retina: Mammalian Retina Metabolism. *Clin. Exp. Ophthalmol.* 2015, 43, 367−376.

(51) Ames, A.; Gurian, B. S. Effects Of Glucose And Oxygen Deprivation On Function Of Isolated Mammalian Retina. *J. Neurophysiol.* 1963, 26, 617−634.

(52) Chertov, A. O.; Holzhausen, L.; Kuok, I. T.; Couron, D.; Parker, E.; Linton, J. D.; Sadilek, M.; Sweet, I. R.; Hurley, J. B. Roles of Glucose in Photoreceptor Survival. *J. Biol. Chem.* 2011, 286, 34700−34711.

(53) Barathi, V. A.; Chaurasia, S. S.; Poidinger, M.; Koh, S. K.; Tian, D.; Ho, C.; Iuvone, P. M.; Beuerman, R. W.; Zhou, L. Involvement of GABA Transporters in Atropine-Treated Myopic Retina As Revealed by ITRAQ Quantitative Proteomics. *J. Proteome Res.* 2014, 13, 4647−4658.

(54) Frost, M. R.; Norton, T. T. Alterations in Protein Expression in Tree Shrew Sclera during Development of Lens-Induced Myopia and Recovery. *Invest. Ophthalmol. Vis. Sci.* 2012, 53, 322−336.

(55) Feng, J.; Li, J.; Wu, L.; Yu, Q.; Ji, J.; Wu, J.; Dai, W.; Guo, C. Emerging Roles and the Regulation of Aerobic Glycolysis in Hepatocellular Carcinoma. *J. Exp. Clin. Cancer Res.* 2020, 39, 126.

(56) Li, Y.; Liu, X.; Wang, C.; Su, Z.; Zhao, K.; Yang, M.; Chen, S.; Zhou, L. Molecular and Clinical Characteristics of ATP1A3-Related Diseases. *Front. Neurol.* 2022, 13, No. 924788.

(57) Liang, H.; Crewther, S. G.; Crewther, D. P.; Junghans, B. M. Structural and Elemental Evidence for Edema in the Retina, Retinal Pigment Epithelium, and Choroid during Recovery from Exper-imentally Induced Myopia. *Invest. Ophthalmol. Vis. Sci.* 2004, 45, 2463−2474.

(58) Crewther, S. G.; Liang, H.; Junghans, B. M.; Crewther, D. P. Ionic Control of Ocular Growth and Refractive Change. *Proc. Natl. Acad. Sci. U.S.A.* 2006, 103, 15663−15668.

(59) Yang, X.-L. Characterization of Receptors for Glutamate and GABA in Retinal Neurons. *Prog. Neurobiol.* 2004, 73, 127−150.

(60) Cheng, Z.-Y.; Wang, X.-P.; Schmid, K. L.; Han, Y.-F.; Han, X.-G.; Tang, H.-W.; Tang, X. GABAB Receptor Antagonist CGP46381 Inhibits Form-Deprivation Myopia Development in Guinea Pigs. *BioMed Res. Int.* 2015, 2015, No. 207312.